MSUCP-29
June 1980

PRESENT STATUS OF THE K-800 MAGNETIC FIELD DESIGN

G. Bellomo, E. Fabrici, D. Johnson, F. Resmini

This note summarizes the present status (May 1980) of the K-800 Magnetic field design, the emphasis being on the changes introduced with respect to the Conceptual Design Report (CDR-BIG BOOK) and their implications on the design of the machine. As of now the magnetic field is realistic enough, and looks satisfactory enough, to warrant a detailed engineering study. It is therefore the purpose of this note to analyze the major issues involved and to underline those aspects which should be carefully considered from the engineering point of view.

We shall discuss the following topics:

1) Overall magnet configuration
2) Outline of magnetic field properties
3) Pole tip geometry
4) Trim coils design
5) Main coils design

1) Overall Magnet Configuration

Two major changes in the general configuration of the magnet have taken place, with respect to the CDR:

a) The coil distance from the median plane has increased from 1.5" to 2" in order to provide more room axially for the extraction elements. Other coil dimensions remain the same, i.e. radial width of 6", total effective coil height 26.5".

b) The tank wall thickness is decreased to 1", the 0.25" radial gap between pole and tank being now between 42.00" and 42.25" in radius. As discussed in more detail later, this change has been forced upon us by the obnoxious effects of said gap on the magnetic field effects, which are very difficult, if not impossible, to properly compensate.

As a consequence, the general yoke structure remains unchanged with respect to the drawing 8-MIY-Z-K of 1/31/80, and in particular all outer dimensions remain unchanged. The modification (a) had already been taken into account in said drawing.

However, modification (b) raises the following issues:

- Is the 1" thickness of the tank wall enough to accomodate the vacuum seal jackets on the top and bottom of the tank itself? This is indeed a considerable departure from the engineering line of the K-500, and should be carefully checked out.
- Is this thickness enough for mechanical stresses (axial stresses mostly) on the tank? Chalk River uses a 20 mm (.787") thick tank, of stainless steel, with a radius roughly like the K-500 tank. The answer to this question seems affirmative, but the

point should be investigated further.

- Should we increase the pole radius to 42" (41" in above mentioned drawing) or adopt different solutions (like having a ring fitted to a 41" pole etc.)? Tentatively one would opt for a pole radius increase, unless considerations of pole pieces weight oppose it (or if changes in the bids for the iron are difficult to make).

The holes present in drawing 8-MIY-A-K of 1/31/80, i.e.

- Center hole, with 10" diameter, starting at 18" from the median plane
- Three R.F. holes, 13" in diameter with center at R=31" have all been taken into account in the present calculations, and shall remain unchanged.

2) Outline of Magnetic Field Properties

It seems appropriate, before discussing the details of the pole tip geometry, to briefly review the overall properties of the magnetic field as it stands now. The operating diagram of the machine is obviously unchanged from the CDR and it is shown in Figure 1 and Figure 2 for reference.

A grid of 35 TRIM calculations, spanning the entire operating range of the cyclotron, has been used to provide the average field as a function of radius. Contributions of shims etc. have then been computed with the CHARGE SHEET program and added to the TRIM field. The latter, however, already includes all major features of the pole tip geometry, i.e. the central hole and R.F. holes, and likewise an estimate of the holes in the yoke for coils supporting links, extraction elements etc.

At an excitation of J_α(lower coil) = 3250 A/cm^2 and J_β(upper coil) = -1000 A/cm^2, i.e. close to the one needed for 200 MeV/n ions, the average field is shown in Figure 3, and compared with the theoretical „best field" to mimimize the trim coil power and achieve isochronism (see the CDR for more details). The disagreement is within 30-40 gauss at most (obviously except in the region up to 6"-7", where we purposedly produce a cone field with the central plug). Differences of this order are negligible at this stage and will easily be adjusted when measurements are available.

Fits to the isochronous field for a number of representative ions over the contour of the operating diagram have been carried out and the results shown in Figure 4.

All values of J_α, J_β, in A/cm^2, trim coil powers and energy for each ion are reported. The minimum negative value of J_β is -1537 A/cm^2, and occurs for the 200 MeV/n ions, while its maximum positive value, 3130 A/cm^2, occurs fro the Z/A=.2, B_o = 47 kgauss ion (bending limit). As for J_α (lower coil) its maximum value is 3595 A/cm^2, ion of 2/A=.32, B_0=47 kgauss, at the crossing of the bending and focusing limits. Trim coil powers are confined to 70 kW with no current exceeding 350 A, which leaves therefore a good margin.

The focusing properties of the field look excellent. For 200 MeV/n particles the minimum ν_2 value previous to extraction is 0.15 when a perfectly isochronous field is used. With acceleration above isochronism in this region ν_2=.20 can easily be acheived. At the transition between the two spirals (R=15") one has indeed an imaginary ν_2 over a range of 1" in radius. This can be over come, as shown in Figure 5, by accelerating above isochronism up to the transition radius and below isochronism afterwards. It has been checked that such a field can be achieved with the trim coils, with no significant power increase, and the resulting minimum ν_2 is 0.15, with a maximum phase shift of 14°.

In summary, the present field looks very satisfactory, and only the most compelling engineering arguments should let us depart significantly from the present pole tips-coils configuration.

3) Pole Tips Geometry

3-a- Center Plug

The center plug is substantially similar to the one designed for the K-500. It extends however up to 18" from the median plane and fits in the 7" diameter hole which is anticipated in the pole tips. At 18" from the median plane starts the larger 10" diameter hole anticipated in the pole and yoke. The sketch of the plug is shown in Figure 6. No problems of any kind are expected.

3-b- Pole Tips

The hill contours are shown in Figure 7 and given numerically in Table I. The basic spiral constant is 1/13 rad/inch, as in CDR. The present design is however more realistic. The hill width is 33° at a radius of 3.5", where the sectors start, and flares progressively up to R=15", where it reaches 46°. This radius is also the transition radius between the two spirals, transition which is now sharp because of easier construction of the pole tips, and trim coils fabrication. The hill width stays constant afterwards at 46°, following the spiral law, up to 38". From 38" the width increases linearly by 2°/inch, and reaches 50° at 40". The increase is only on one side of the hill, namely the entrance edge as seen by the particles, in order to locally increase the spiral angle. The width increase has however the principal goal of increasing locally the average field, in order to meet the requirements of the theoretical "best field" (see Figure 3). From a radius of 40.5" and up to 42" the hill is cut radially to a constant width of 50°, in order to decrease the axial focusing and therefore push the $\nu_R + 2\nu_Z=3$ resonance away from the extraction radius of 40.5". It should be stated at this point that the hill configuration between 38" and 42" is not completely finalized yet. Calculations are underway to determine the optimum inital radius of the radial cut, which could conceivably start as early as 40", and the minimum required increase of the spiral between 38" and 40". In any case, the width increase of the hill, as described, will not change because it is entirely determined by average field conditions. Calculations have shown that the other method of producing a similar field increase, namely adding shims to the hill, would lead to gap reductions of 200-250 mils, which would dangerously reduce the axial space needed for the deflectors. It is conceded that this method will entail a local reduction of 4^{o} of the gap to gap angular width otherwise available. The expected reduction still allows use of about 95% of the peak dee voltage, which does seem quite acceptable.

Three large holes are anticipated in each valley:

- at R=21", diameter 5" for a trimming capacitor
- at R=31", diameter 13" for the dee stem
- at R=36", diameter 5" for the coupling capacitor.

There are in addition 22 x 2 = 44 holes on the side of each hill, for the leads of the 22 anticipated trim coils. Needless to say, the calculations have taken into account all the holes. The radial profile of a hill and a valley is shown in Figure 8. For the hill the major difference with respect to CDR is an increase in thickness, to 9.75", in order to increase the flutter. The valley is shimmed, with an 8" thick shim from R=3.5" to R=7", 2" thick from 7" to 14", 1.5" thick from 14" to 24" and .75" from 24" to 31". A valley skirt, between 41" and 42", extending up to 5" from the median plane is also needed, and existed already in CDR.

The hill is chamferred, as in the K-500, but tentatively the amount of chamfering has been reduced to one half that of the K-500. The iron part of the tank wall from 41.25" to 42.25", extends up to 2.25" from the median plane, as in CDR.

3-c- Design implications

The engineering study of the presently proposed configuration should clarify the following points:

- Minimum number of parts in which the hills should be split. Obviously two is a bare minimum. The requirements of conserving some flexibility in the range between 38" and 42" in radius (where, as in all edge-regions, a final disign could probably exist only after magnetic field measurements) suggests that three or even four sections--splitting may be a desirable option. In any case provisions should be made for easy edge-profile corrections in the above mentioned radial range
- Hill chamfering. The reduction by a factor of two in the hill chamfering, with respect to the K-500, brings about a flutter increase and has therefore been tentatively selected. It is however recognized that such a reduction might involve several problems in: i) bending to a smaller curvature radius the trim coils cable. ii) getting a linear-cooling duct in the space between the liner and the trim coils. Should this option be

judged too marginal for the above issues, it is our opinion that we could fall back to a K500-like chamfering without unbearable consequences on the magnetic field properties.

- Pole tips thickness. The present pole tips thickness of 9.25" should not be decreased, by any means. It is realized that in the radial range of 3.5" to 7" (see Figure 8) the 8" thick valley shim will interfere with the wrapping of the three coils around the hill. We propose that in this region the valley shim is split axially into two parts: one up to 11.62" from the median plane, thus leveling with the lower hill part; the second will have an azimuthal width decreased by about 1" on either side, to allow for trim coils insertion, and will be bolted to the first when trim coils assembly is completed. The thickness of this second part, nominally of 1.6", will have to be increased by about 25% in order to preserve the total volume of iron.
- Valley shims. They seem to pose no particular problem, except for the 1" thick shim between R=41" and R=42". If the decision is made to increase the pole radius to 42", then provisions have to be made for fabricating and properly fastening such a tall, thin, shim to the polar structure. If some other option looks more attractive, like fitting a ring to a 41" pole, then one should carefully consider the interaction of such a ring with the sectors geometry.

The interaction between the 0.75" shim from R=24" to R=31" and the R.F. hole (dee stem) centered at R=31" is unimportant and does not constitute any design problem.

- Position of the R.F. holes for the turning and coupling capacitors. Their effect on the field is quite smooth and provided there is not a drastic change in the radial position they can be shifted around, in the future, depending upon the results from the forthcoming 1:2 R.F. model.
- Transition between the two spirals at R=15". The sharp transition works all right and we should stick to the present disign.

4) Trim Coils Design

As stated above, 22 trim coils are anticipated. For the sake of easy computation they have been represented as equally spaced in radius, the interval being .3", and 1.4" wide radially, i.e. approximately as in the K-500. Their radial positions are listed in Table II. A more realistic trim coil pattern should now be devised, taking into account the need for the supports beneath the upper hill part, and for spaces between the trim coils themselves. In particular:

- The 22nd trim coil, i.e. the outer one, should be moved inwards from its present outer radius of 40.8". The reason is that extraction will take place, as mentioned before, at about 40.5". For 200 MeV/n ions, it has already been checked that an outer radius of 40.2" will not limit the trim coils ability to fit the desired field (fitting radius = 38.5"). We recommend that this outer radius be selected as a basis, in order not to interfere with the deflectors in their predictable inwards movement of .2" when less relativistic ions are used.

Table II

TRIM COIL RADII

TC#	R_1	R_2
1	3.7	5.1
2	5.4	6.8
3	7.1	8.5
4	8.8	10.2
5	10.5	11.9
6	12.2	13.6
7	13.9	15.3
8	15.6	17.00
9	17.3	18.7
10	19.00	20.4
11	20.2	22.1
12	22.4	23.8
13	24.1	25.5
14	25.8	22.2
15	27.5	28.9
16	29.2	30.6
17	30.9	32.3
18	32.6	34.00
19	34.4	35.7
20	36.0	37.4
21	37.7	39.1
22	39.4	40.8

- If absolutely necessary for reasons of spacers between the trim coils, and/or of pole tips supports, the number of trim coils could be reduced from 22 to 21 without probably jeopardising the overall fit performance as outlined in 2). However this should be considered as a "last resort" option since the lower the number of trim coils the higher are the oscillations induced by them around the isochronous field. Consequently, larger oscillations in ν_z can be expected. If such an option is envisaged, the reduction in the trim coil number should take place preferably in the radial range of 20" to 35", where ample axial focusing is available. By no means should the "density" of trim coils be reduced between 35" and 50", where the actual minimum in ν_Z occurs.

- Another option, and which is by far the most attractive one, should be mentioned. It consists in increasing the hill gap from the present 2.5" to 3". The resulting flutter decrease should not bother us over most radii, since there we have ample flutter margins. The only critical region is where the minimum ν_Z is reached, i.e. around a radius of 37.5" - 38.5". Here however a local spiral increase of $\simeq 1^{\circ} - 2^{\circ}$, and/or reduction in the size of the radial cut (see par 3.b) should in principle allow one to maintain a reasonable ν_Z value.

  Under this hypothesis (which will be tested shortly) one has the following design scenario:

  i) The last two trim coils, covering the radial range (Table II) from 37.7" to 40.8" are made of one layer only. The current obviously doubles, but it would not be higher than 550-600 amps. Such a single layer trim coil could certainly be built to occupy ≃1/4" or thereabout axially.

  ii) The electrostatic deflector would then have the full (or thereabout) 2.5" axial clearance even if it had to move above the trim coils.

  iii) We would not have to worry too much, then, over the $\nu_R + 2\nu_Z = 3$ resonance (see CDR) restricting our operating range at low fields. Since low field beams are not at all difficult to extract, we could just move the deflector inwards, readially, in order to extract them before they hit the resonance. The anticipated radial moving range is of the order of ≃.6", i.e double that of the K-500, which does not seem to pose any serious problem.

- The "theoretical" trim coils are supposedly fabricated with the same conductor as in the K-500, i.e. 1/4" square hollow conductor. No investigation is therefore necessary on this side.

5) Main Coils Design

5-a-General Considerations

Let us recall briefly the overall coils dimensions: the total coil height of 26.5" is split into a lower coil, closer to the median plane, of fractional height .6, and an upper one of fraction .4. Consequently the lower coil extends from 2" up to 18" distance from the median plane, the upper one from 18.5" to 28". The coils inner radius is 45.5", the outer one 51.5", i.e. 6" in radial width. Assuming a maximum design value for the current density in both coils sections, of 3500 A/cm^2 (although such a density, as shown in Figure 4 will never occur simultaneously in both) one has:

- max ampereturns in the lower coil = 2.16810^6
- max ampereturns in the upper ocil = 1.42210^6

There values have to be multiplied by 2 if the <u>total</u> number of ampere turns is desired.

As of now an appropriate conductor section looks like 1.4" x 1/8". With such a choice a promising geometry is:

- Lower coil: 36 radial layers, total radial width, including G10 pickets and mylar, Of 6.08". 64 turns for each layer, total number of turns = 2304.
- Upper coil: 42 turns for each layer, total number of turns = 1512.

These coils would provide the design number of ampereturns with a current of I = 941 A.

Under these assumptions the conductor length needed is:
Lower coil = 17.840 m x 2 = 35.680 m
Upper coil = 11.710 m x 2 23.420 m
the total length being therefore 59.1 km.

The energy stored in the magnet at the design current density of 3500 A/cm^2 in both coils in approximately 60 MJ. (An error has been uncovered, in this aspect, in the CDR, namely that the values given in Table II.3, page 36, had not been multipled by two as required after a TRIM calculation.) With 60 MJ and a current of, say, 1000 A, the total inductance will be 120H. This compares with 70H in the K-500 magnet, at a stored energy of 17 MJ.

This possible coil design should be further investigated in order to select a final conductor. These points have to be checked:

- coil winding problems, i.e. lathe to be used, its feeding thread, etc.
- is it advisable to go to a higher nominal current, i.e. I>1000A? This should be considered in connection to the charging time of the magnet, and a first estimate of the dump resistor characteristics and discharging time.

Incidentally, we should also decide either to pursue a three feedthrough design, as in the K-500, or go to a four feedthrough solution. Since in the K-800 the upper coil runs negative, the central "tap" will carry in that instance the sum of the currents, instead of the difference as in the K=500. The worst case happens for the 200 MeV/n, see Fig. 4. If we use the present figures for the conductor size the max current for the central "tap" would be $(\frac{3500 + 1500}{3500}) \times 940 = 1340$ A

5-b) Forces and Stresses

These have been computed using as a basis the magnetic field in the coil region obtained in TRIM calculations. As could be expected, the limiting cases turn out to be, in every instance, the 3500/3500 A/cm^2 and the 3500/-1500 A/cm^2.

In the first case both coils sections are attracted toward the median plane, the upper one with a total force of ≃2250 tons the lower one with just ≃230 tons. In the second case, i.e. $J_\alpha = 3500$ and $J_\beta = -1500$ A/cm^2, the upper coil is subject to a force away from the median plane of 905 tons, while the lower one is still attracted toward the median plane with ≃2128 tons. The contours of constant axial force across the coils, in terms of kilograms per meter of cable length, are shown for both cases in Figure 9 and 10. The cable used in these calculations is obviously the one described earlier, i.e. with a nominal current of 941 A at 3500 A/cm^2.

Under the hypothesis of a picket fence construction like the one used in the K-500, i.e. .5" wide pickets at 0.5" azimuthal intervals, one can quickly estimate the radial compressive stress needed in the coils to absorb the axial force through friction. This is given by

$$\sigma_R \geqslant \frac{R}{S_{picket}} \times \mu$$

, where μ is the friction coefficeint and S the area covered by the pickets per meter of cable. Using the numbers given above, and assuming $\mu = .2$, one obtains $\sigma_R \geqslant$(psi) 1.12 F if F is expressed, as in the Figures 9 and 10, in Kg/m.

Radial σ_R and hoop σ_O stresses have been computed , for the two limiting cases, using a home-made program based upon analytical solutions to the stress equations. The program computes separately the three different phases of coil operation, i.e. initial winding at room temperature, cool down, and turning the magnetic field on. Checked against the data for the K-500 coils, as obtained by "exact" calculations, it reproduces the stresses generally quite well, i.e. within 10%. Larger errors of about 20%, are observed for the radial stress near the bobbin mostly in the winding and preload phases, the error being in the sense of underestimating σ_R. The field-on effects are instead very well reproduced both for σ_R and σ_O. In summary, the program can be used with some confidence at least for a preliminary coil design.

The data for the K800 coil are shown in self explanatory ways in Figures 11 through 16, for both limiting cases.

The bobbin is assumed 1" thick from 45.5" to 45.5" in radius. The preload for the cable is of 3000 psi, and for the aluminum banding, 2" thick, of 20.000 psi.

In the 3500/3500 case, the only reason of concern could be that the σ_R tends to be very small, Fig. 11 when the the field is on, in the vicinity of the bobbin. If one takes into account the 20% underestimate of σ_R, mentioned above, for the preload and cool down, one gets more comfortable values of σ_R, i.e. $-1.3\ 10^2$ psi and -1.5 psi, for the lower and upper coil respectively. This should however be checked with a more exact program. A similar problem could exist, in the 3500/-1500 case, for the lower coil only (Fig. 13). Again the minimum σ_R at the bobbin could be -2.410^2 psi.

The hoop stress does not look critical in either case, if a 15.000 psi "safe limit" is assumed for the cable.

In summary, this review of forces and stresses in the K800 coils indicates that the following points should be given particular attention:

- Cryostat structure in order to dispose of the forces on the coils transmitted by the picket fences. Especially the upper part of the cryostat, given the 900 tons force exerted by the upper coil section should be looked into in some detail. We recall that this feature is quite novel compared to the K500 coils.
- More exact calculations of the stresses must be carried out when the coil design, including the conductor choice is finalized.
- Given the forces exerted on the median plane spaces between the coils, one must estimate the maximum size of the holes which can be predicted for the insertion of the extraction elements, and for the passage of the injected beams.

TABLE I

FINAL PROFILES

SPIRAL COSTANT 13.000

TRANS. RADIUS 15.000

TRANS. WIDTH .000

R	HILL N. 1		HILL N. 2		HILL N.
3.50	-133.30	-100.30	-13.30 ✓	19.70 -	106.70
4.00	-131.07	-96.64	-11.07 ✓	23.36 -	108.93
5.00	-127.06	-90.53	-7.06 ✓	29.47 -	112.94
6.00	-123.37	-85.29	-3.37 ✓	34.71 -	116.63
7.00	-119.83	-80.50	.17 ✓	39.50 -	120.17
8.00	-116.35	-75.95	3.65 ✓	44.05 -	123.65
9.00	-112.88	-71.51	7.12 ✓	48.49 -	127.12
10.00	-109.49	-66.98	10.51 ✓	53.02 -	130.51
11.00	-105.81	-62.60	14.19 ✓	57.40 -	134.19
12.00	-102.00	-58.10	18.00 ✓	61.90 -	138.00
13.00	-98.01	-53.41	21.99 ✓	66.59 -	141.99
14.00	-93.76	-48.46	26.24 ✓	71.54 -	146.24
15.00	-89.11	-43.11	30.89 ✓	76.89 -	150.89
15.00	-89.11	-43.11	30.89 ✓	76.89 -	150.89
15.50	-91.31	-45.31	28.69	74.69	148.69
16.00	-93.52	-47.52	26.48 +	72.48 -	146.48
16.50	-95.72	-49.72	24.28	70.28	144.28
17.00	-97.93	-51.93	22.07 +	68.07 -	142.07
17.50	-100.13	-54.13	19.87	65.87	139.87
18.00	-102.33	-56.33	17.67 +	63.67 -	137.67
18.50	-104.54	-58.54	15.46	61.46	135.46
19.00	-106.74	-60.74	13.26 -	59.26 -	133.26
19.50	-108.94	-62.94	11.06	57.06	131.06
20.00	-111.15	-65.15	8.85 -	54.85 -	128.85
20.50	-113.35	-67.35	6.65	52.65	126.65
21.00	-115.55	-69.55	4.45 -	50.45 -	124.45
21.50	-117.76	-71.76	2.24	48.24	122.24
22.00	-119.96	-73.96	.04 -	46.04 -	120.04
22.50	-122.17	-76.17	-2.17	43.83	117.83
23.00	-124.37	-78.37	-4.37 -	41.63 -	115.63
23.50	-126.57	-80.57	-6.57	39.43	113.43
24.00	-128.78	-82.78	-8.78 -	37.22 -	111.22
24.50	-130.98	-84.98	-10.98	35.02	109.02
25.00	-133.18	-87.18	-13.18 -	32.82 -	106.82
25.50	-135.39	-89.39	-15.39	30.61	104.61
26.00	-137.59	-91.59	-17.59 -	28.41 -	102.41
26.50	-139.80	-93.80	-19.80	26.20	100.20
27.00	-142.00	-96.00	-22.00 -	24.00 -	98.00
27.50	-144.20	-98.20	-24.20	21.80	95.80
28.00	-146.41	-100.41	-26.41 -	19.59 -	93.59
28.50	-148.61	-102.61	-28.61	17.39	91.39

TABLE I (continued)

29.00	-150.81	-104.81	-30.81	15.19	89.19
29.50	-153.02	-107.02	-33.02	12.98	86.98
30.00	-155.22	-109.22	-35.22	10.78	84.78
30.50	-157.42	-111.42	-37.42	8.58	82.58
31.00	-159.63	-113.63	-39.63	6.37	80.37
31.50	-161.83	-115.83	-41.83	4.17	78.17
32.00	-164.04	-118.04	-44.04	1.96	75.96
32.50	-166.24	-120.24	-46.24	-.24	73.76
33.00	-168.44	-122.44	-48.44	-2.44	71.56
33.50	-170.65	-124.65	-50.65	-4.65	69.35
34.00	-172.85	-126.85	-52.85	-6.85	67.15
34.50	-175.05	-129.05	-55.05	-9.05	64.95
35.00	-177.26	-131.26	-57.26	-11.26	62.74
35.50	-179.46	-133.46	-59.46	-13.46	60.54
36.00	-181.67	-135.67	-61.67	-15.67	58.33
36.50	-183.87	-137.87	-63.87	-17.87	56.13
37.00	-186.07	-140.07	-66.07	-20.07	53.93
37.50	-188.28	-142.28	-68.28	-22.28	51.72
38.00	-190.48	-144.48	-70.48	-24.48	49.52
38.50	-193.68	-146.68	-73.68	-26.68	46.32
39.00	-196.89	-148.89	-76.89	-28.89	43.11
39.50	-200.09	-151.09	-80.09	-31.09	39.91
40.00	-203.29	-153.29	-83.29	-33.29	36.71
40.50	-205.50	-155.50	-85.50	-35.50	34.50
41.00	-205.50	-155.50	-85.50	-35.50	34.50
41.50	-205.50	-155.50	-85.50	-35.50	34.50
42.00	-205.50	-155.50	-85.50	-35.50	34.50

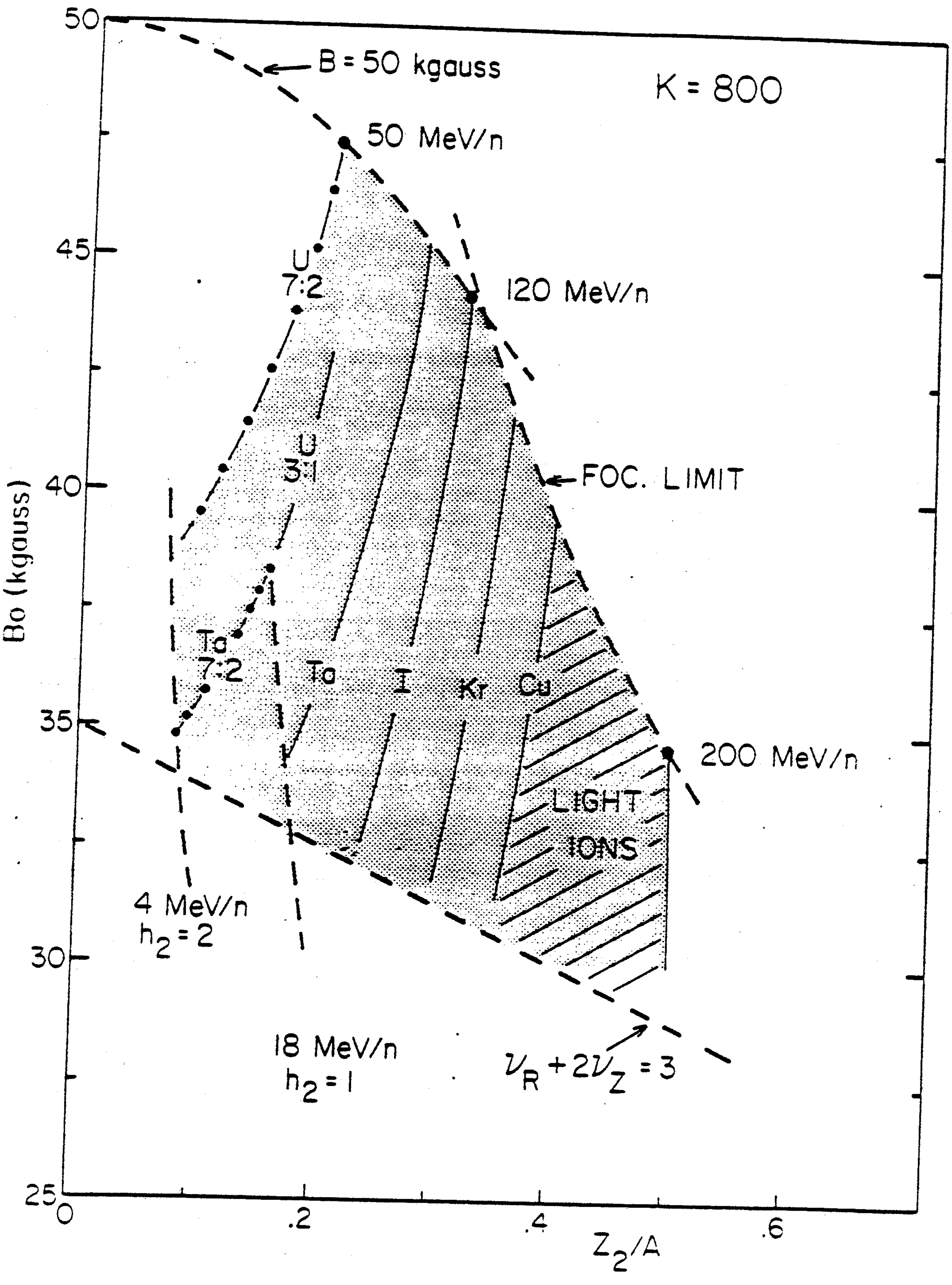

B = 50 kgauss
K = 800
50 MeV/n
120 MeV/n
200 MeV/n
FOC. LIMIT
U 7:2
U 3:1
Ta 7:2
Ta
I
Kr
Cu
LIGHT IONS
4 MeV/n $h_2 = 2$
18 MeV/n $h_2 = 1$
$\nu_R + 2\nu_Z = 3$
Bo (kgauss)
Z_2/A
50
45
40
35
30
25
0
.2
.4
.6

Figure 1

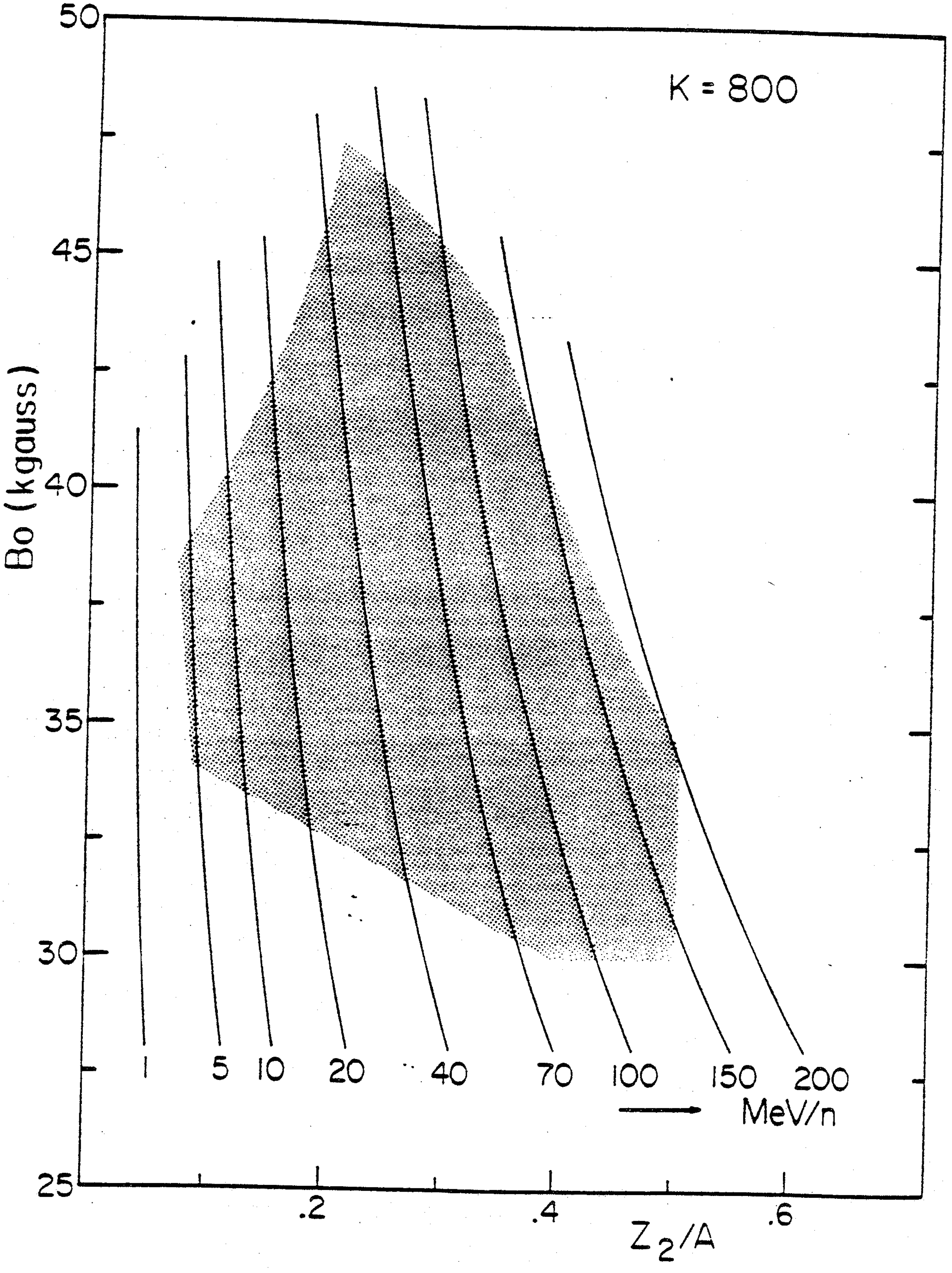

K = 800
Bo (kgauss)
50
45
40
35
30
25
1
5
10
20
40
70
100
150
200
MeV/n
.2
.4
.6
Z2/A

Figure 2

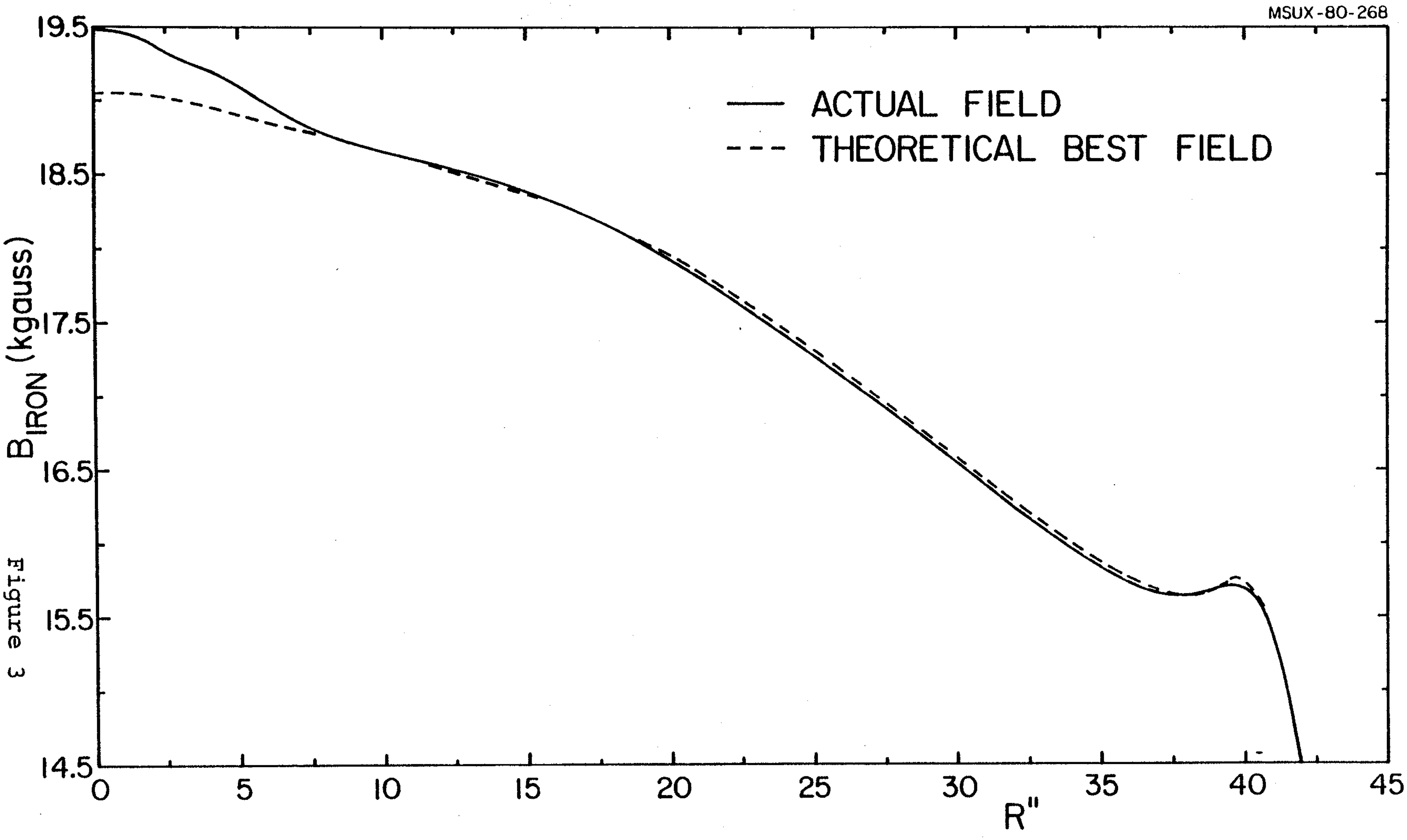
MSUX-80-268
ACTUAL FIELD
THEORETICAL BEST FIELD
B_{IRON} (kgauss)
19.5
18.5
17.5
16.5
15.5
14.5
0
5
10
15
20
25
30
35
40
45
R"

Figure 3

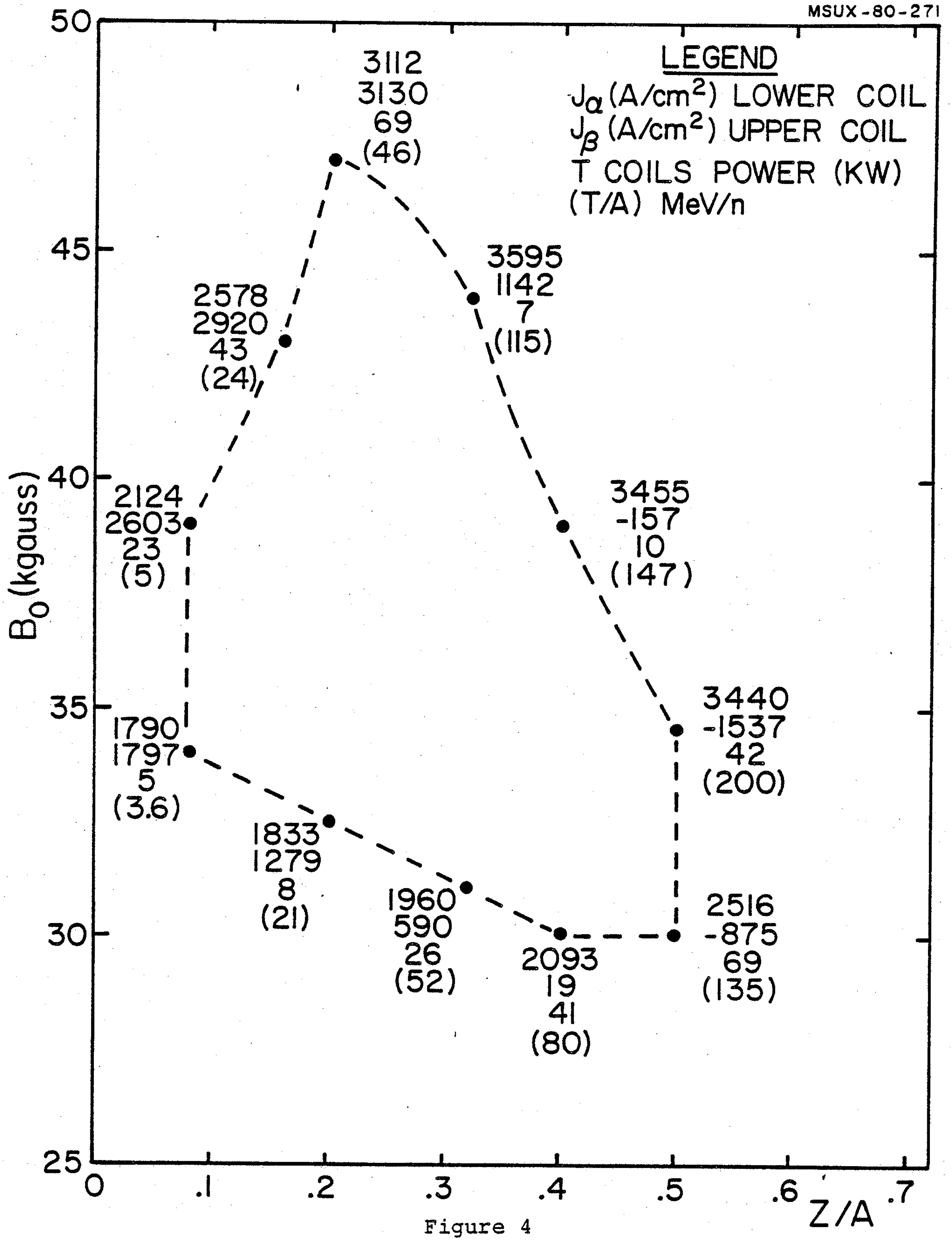
MSUX-80-271
LEGEND
J_α (A/cm^2) LOWER COIL
J_β (A/cm^2) UPPER COIL
T COILS POWER (KW)
(T/A) MeV/n
B_0 (kgauss)
Z/A
50
45
40
35
30
25
0
.1
.2
.3
.4
.5
.6
.7
3112
3130
69
(46)
2578
2920
43
(24)
3595
1142
7
(115)
2124
2603
23
(5)
3455
-157
10
(147)
1790
1797
5
(3.6)
3440
-1537
42
(200)
1833
1279
8
(21)
1960
590
26
(52)
2093
19
41
(80)
2516
-875
69
(135)

Figure 4

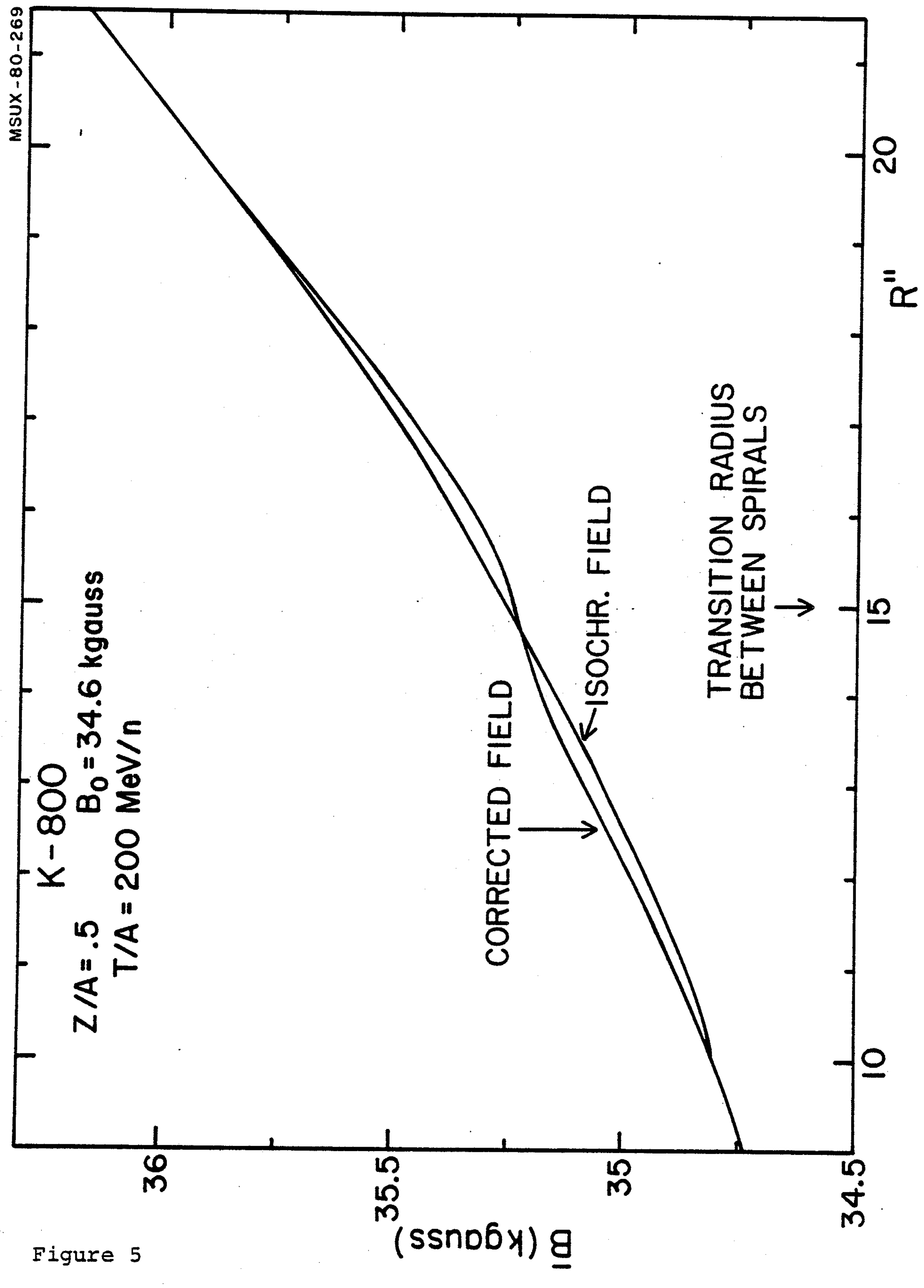
MSUX-80-269
K-800
Z/A = .5
B_o = 34.6 kgauss
T/A = 200 MeV/n
CORRECTED FIELD
ISOCHR. FIELD
TRANSITION RADIUS
BETWEEN SPIRALS
B (kgauss)
36
35.5
35
34.5
R"
10
15
20

Figure 5

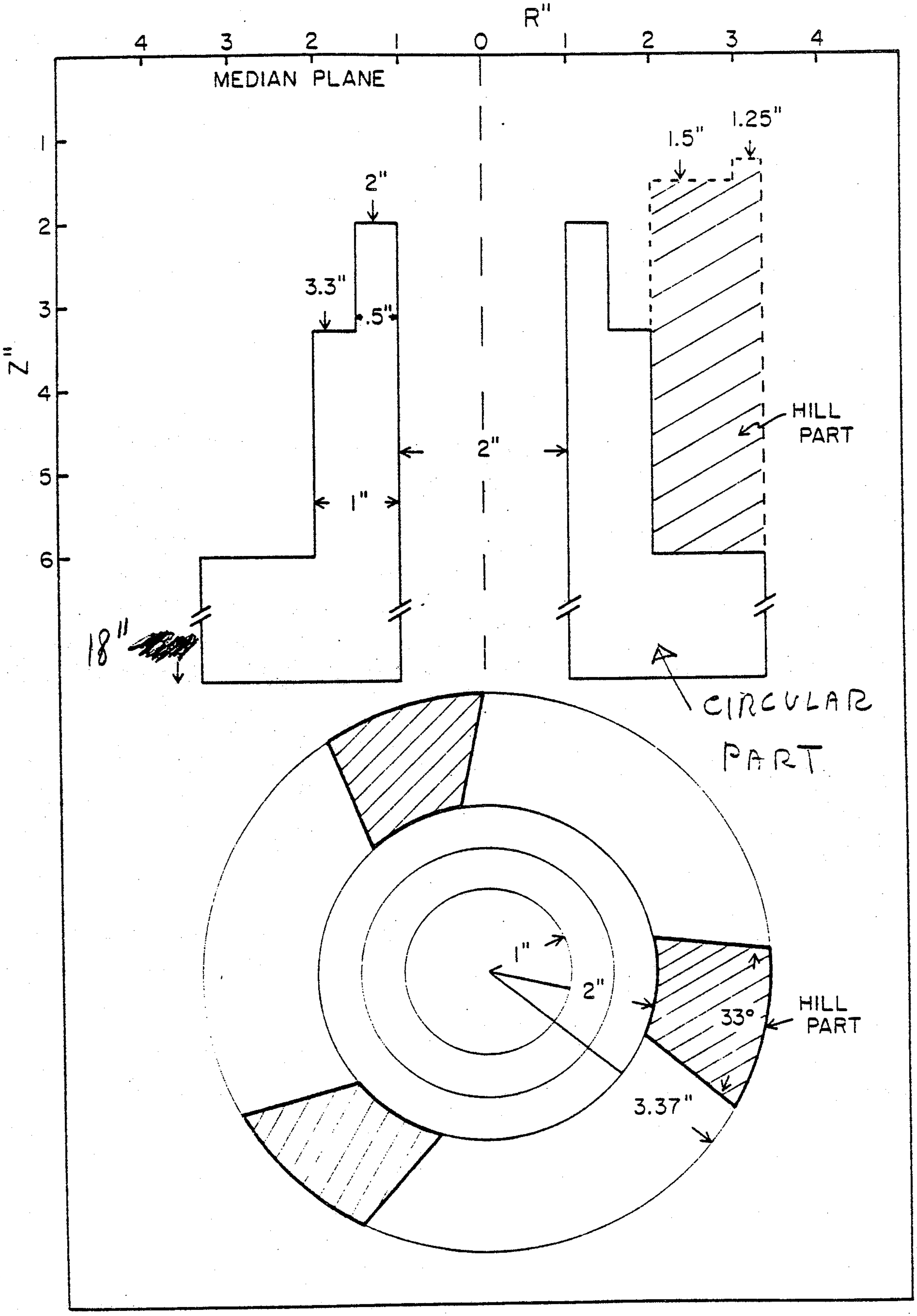
R"
4
3
2
1
0
1
2
3
4
MEDIAN PLANE
Z"
1
2
3
4
5
6
1.25"
1.5"
2"
3.3"
.5"
2"
1"
HILL PART
18"
CIRCULAR PART
1"
2"
33°
HILL PART
3.37"

Figure 6

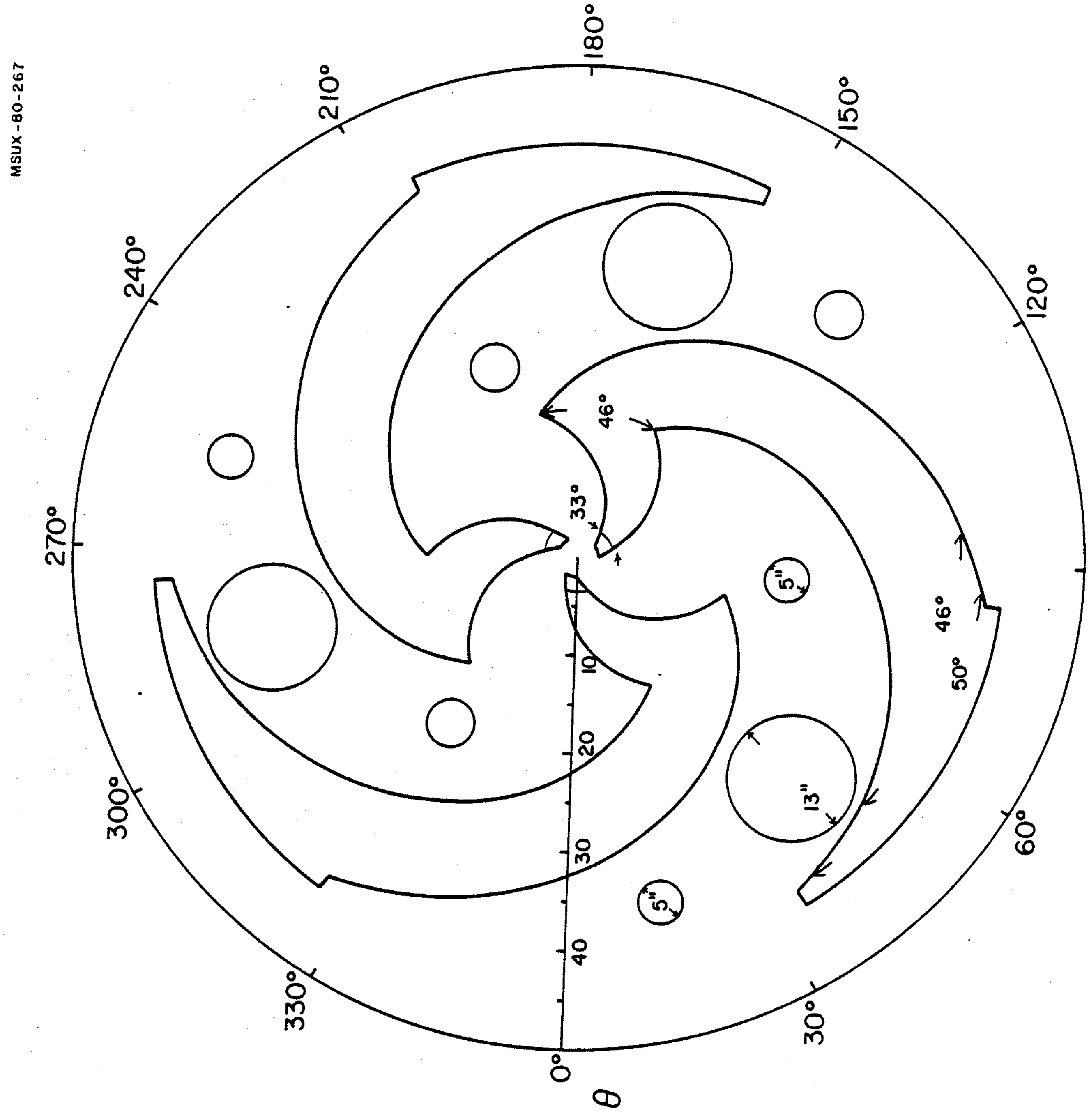
MSUX-80-267
180°
210°
150°
240°
120°
270°
90°
300°
60°
330°
30°
0°
θ
10
20
30
40
33°
46°
46°
50°
5"
5"
13"

Figure 7

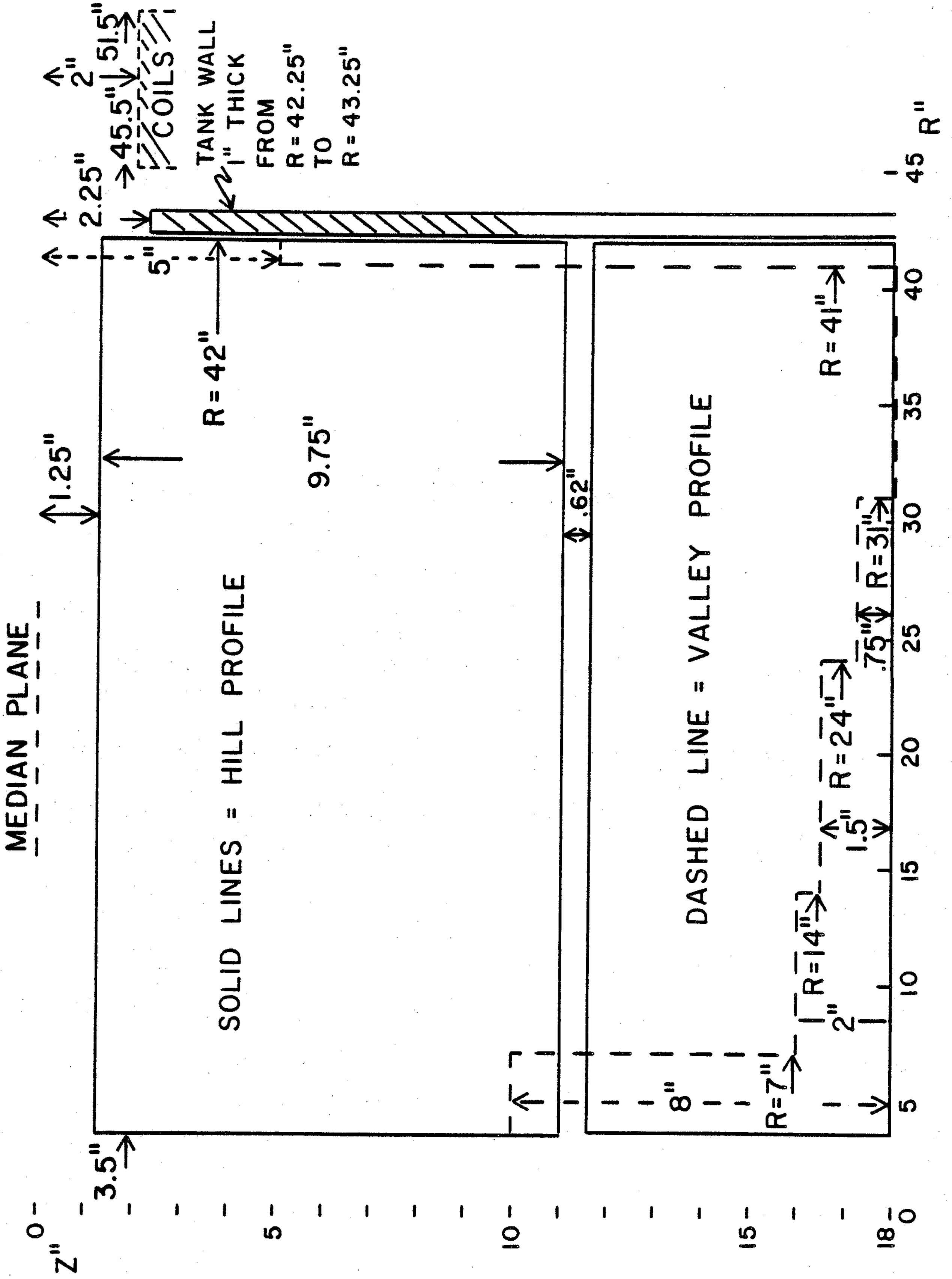
MEDIAN PLANE
SOLID LINES = HILL PROFILE
DASHED LINE = VALLEY PROFILE
TANK WALL
1" THICK
FROM
R = 42.25"
TO
R = 43.25"
COILS
45.5"
51.5"
2"
2.25"
5"
R = 42"
1.25"
9.75"
.62"
R = 41"
R = 31"
.75"
R = 24"
1.5"
R = 14"
2"
R = 7"
8"
3.5"
Z"
R"
0
5
10
15
18
20
25
30
35
40
45

Figure 8

MSUX-80-272

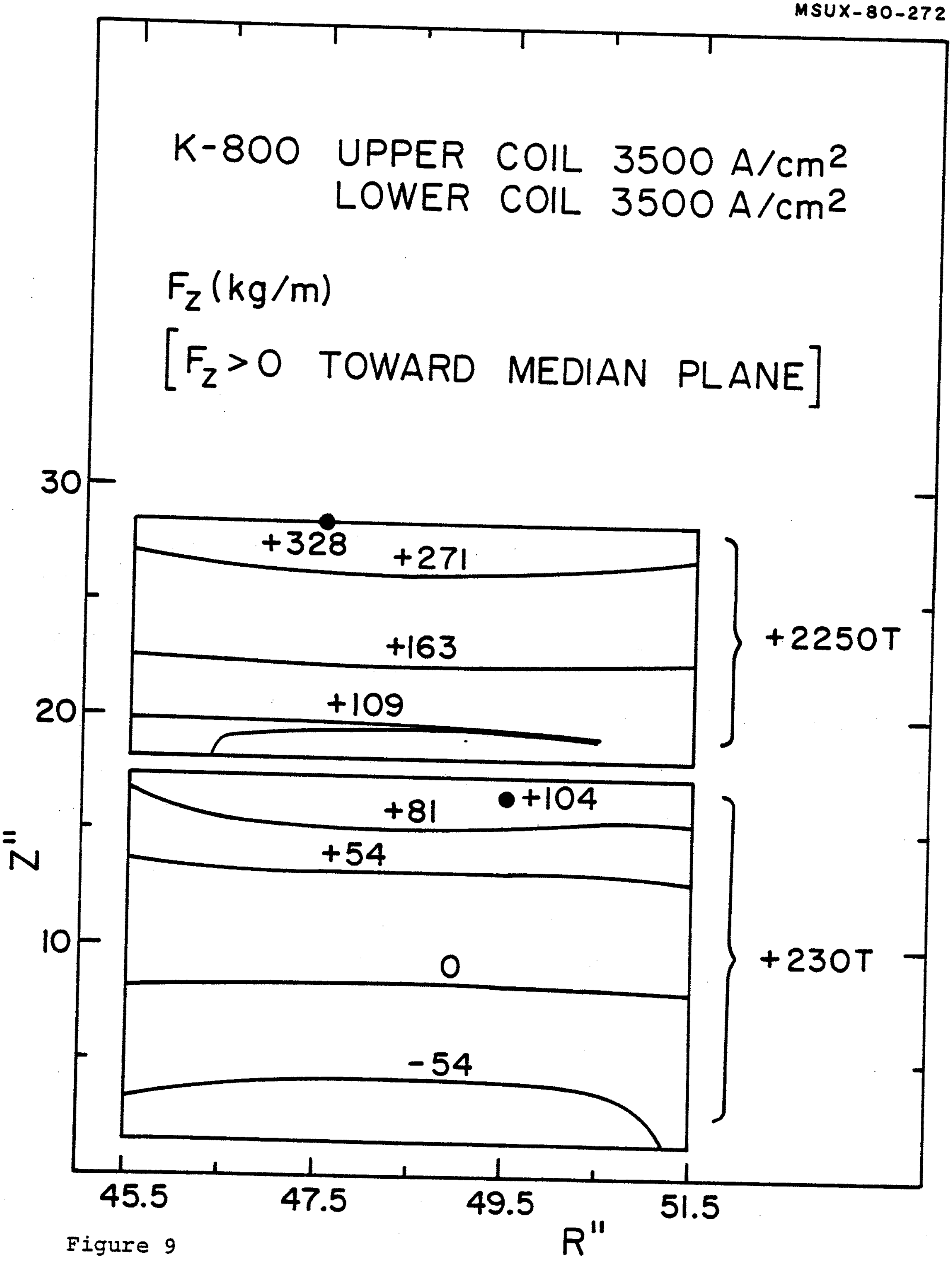

Figure 9

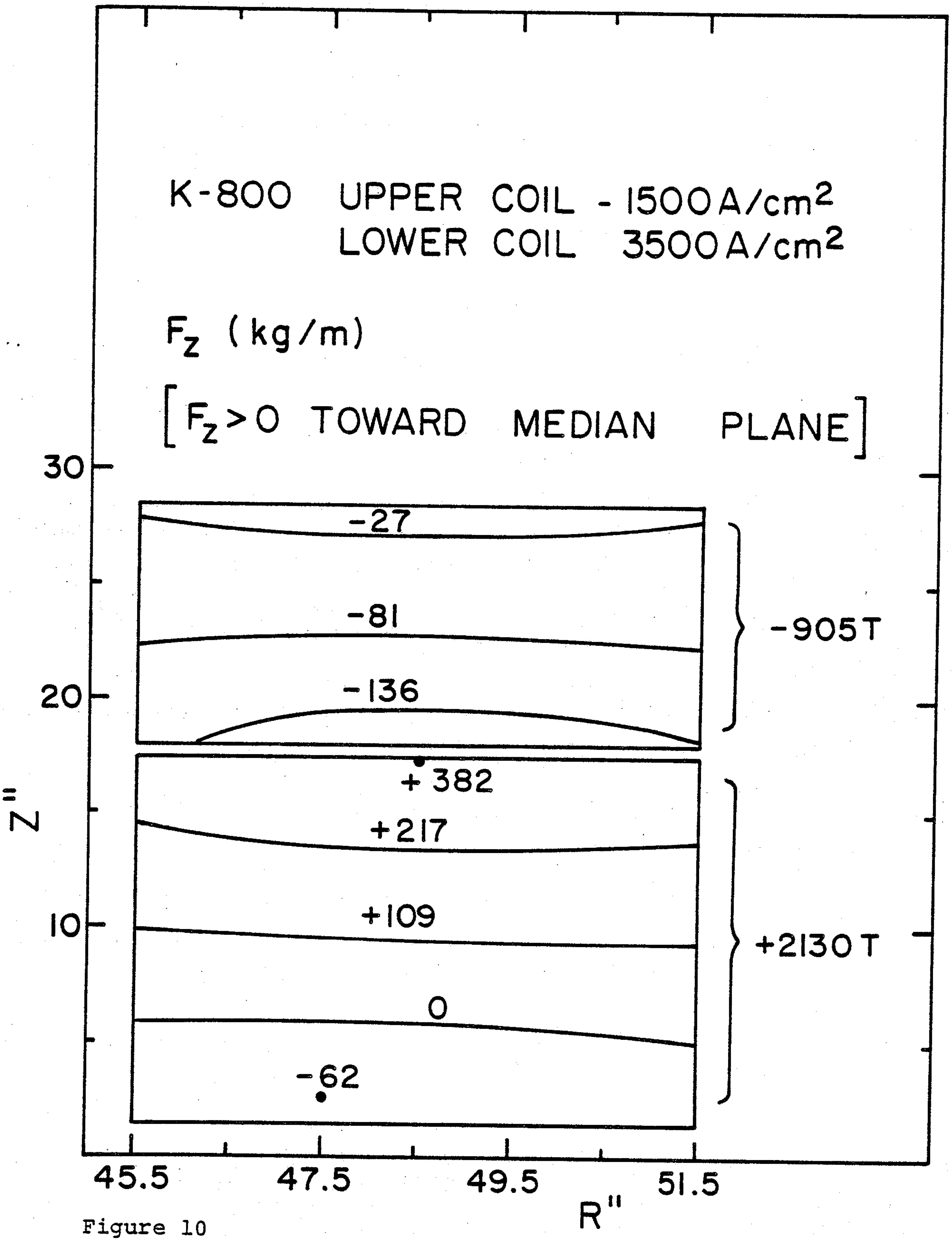
K-800 UPPER COIL -1500 A/cm2
LOWER COIL 3500 A/cm2
Fz (kg/m)
[Fz>0 TOWARD MEDIAN PLANE]
-27
-81
-136
-905T
+382
+217
+109
0
-62
+2130T
30
20
10
Z"
45.5
47.5
49.5
51.5
R"

Figure 10

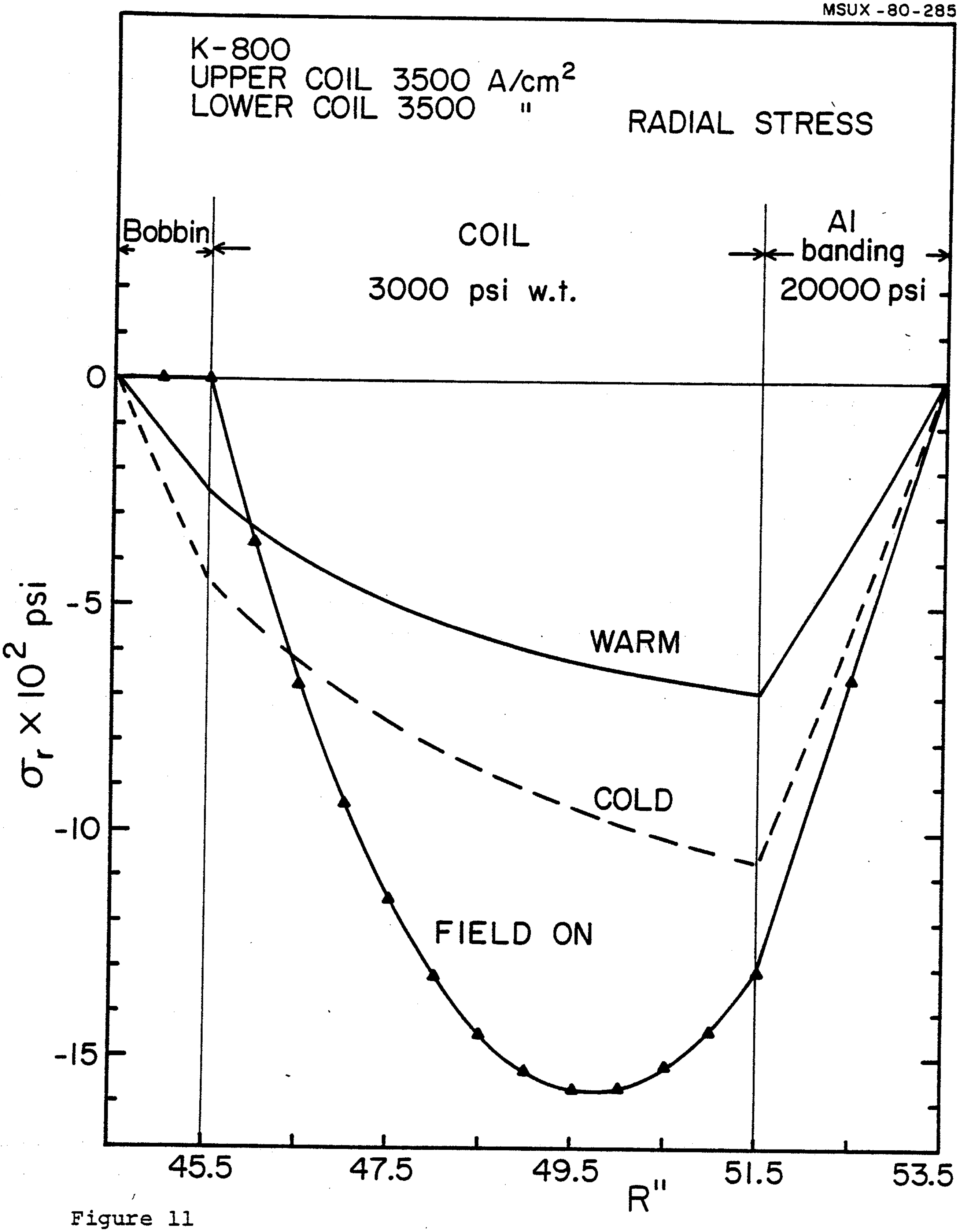
K-800
UPPER COIL 3500 A/cm²
LOWER COIL 3500 "
RADIAL STRESS
Bobbin
COIL
3000 psi w.t.
Al banding
20000 psi
WARM
COLD
FIELD ON
0
-5
-10
-15
σr × 10² psi
45.5
47.5
49.5
51.5
53.5
R"

Figure 11

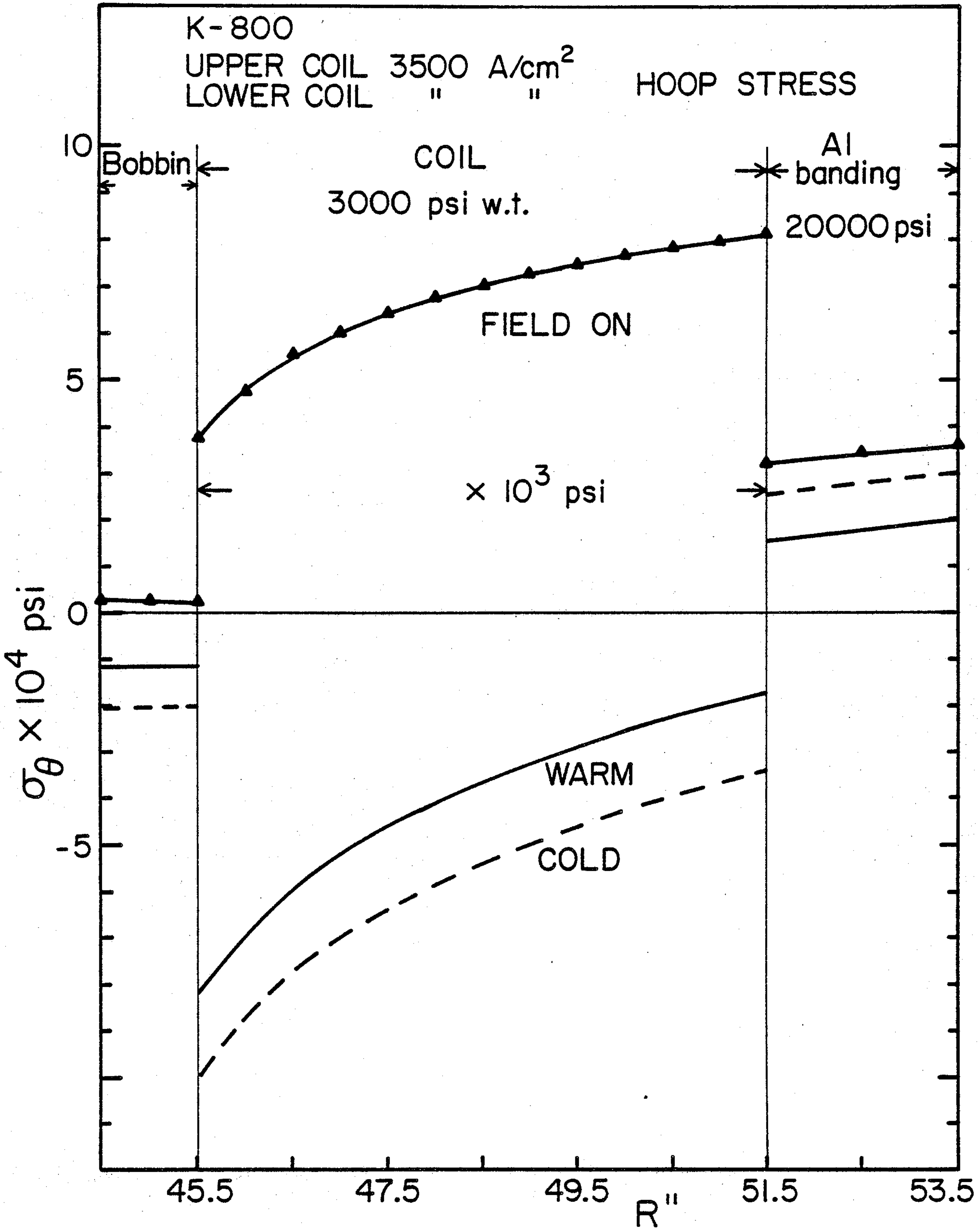
K-800
UPPER COIL 3500 A/cm²
LOWER COIL " "
HOOP STRESS
Bobbin
COIL
3000 psi w.t.
Al banding
20000 psi
FIELD ON
× 10³ psi
WARM
COLD
σθ × 10⁴ psi
10
5
0
-5
45.5
47.5
49.5
51.5
53.5
R"

Figure 12

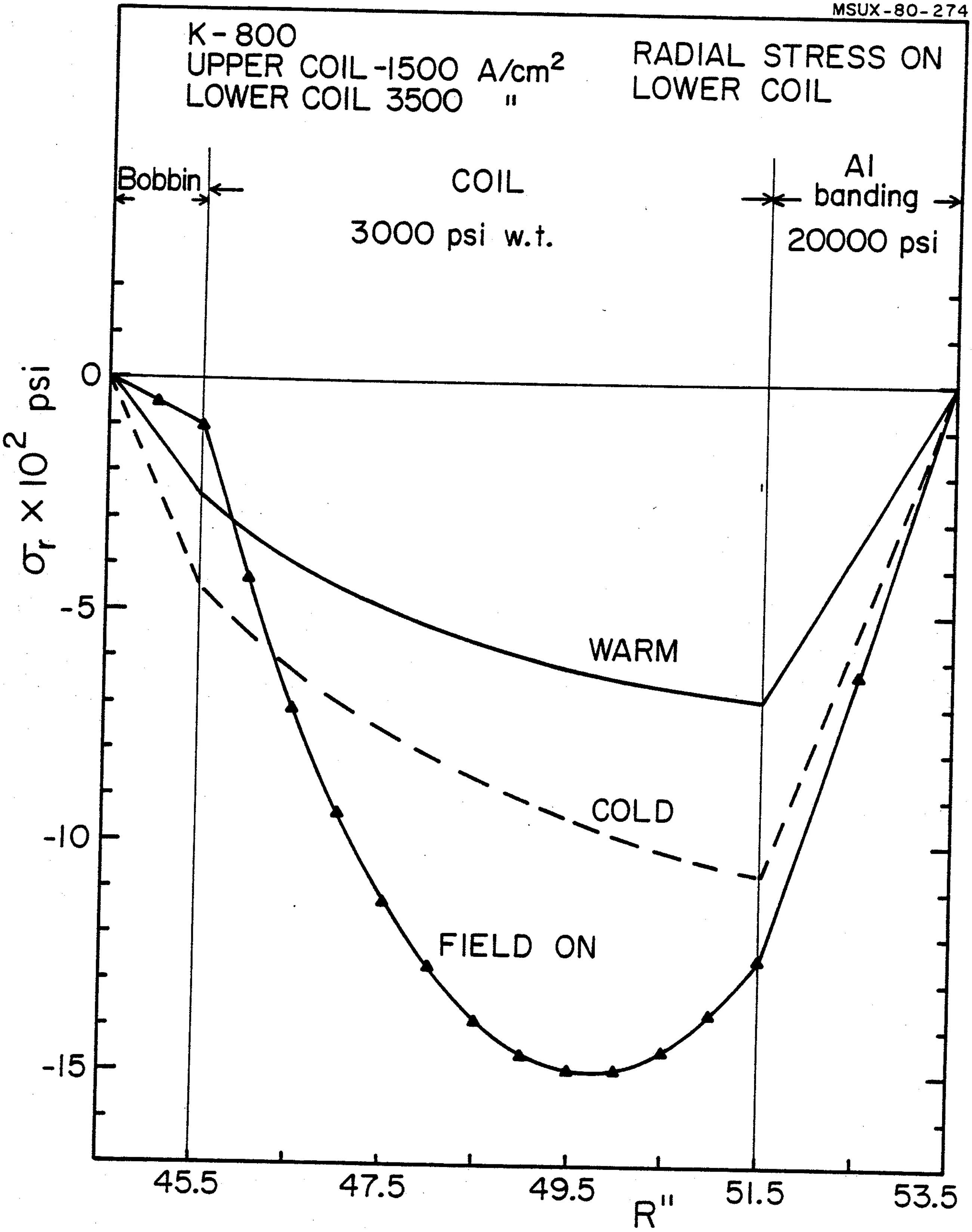
MSUX-80-274
K-800
UPPER COIL-1500 A/cm²
LOWER COIL 3500 "
RADIAL STRESS ON LOWER COIL
Bobbin
COIL
3000 psi w.t.
Al banding
20000 psi
WARM
COLD
FIELD ON
σr × 10² psi
0
-5
-10
-15
45.5
47.5
49.5
51.5
53.5
R"

Figure 13

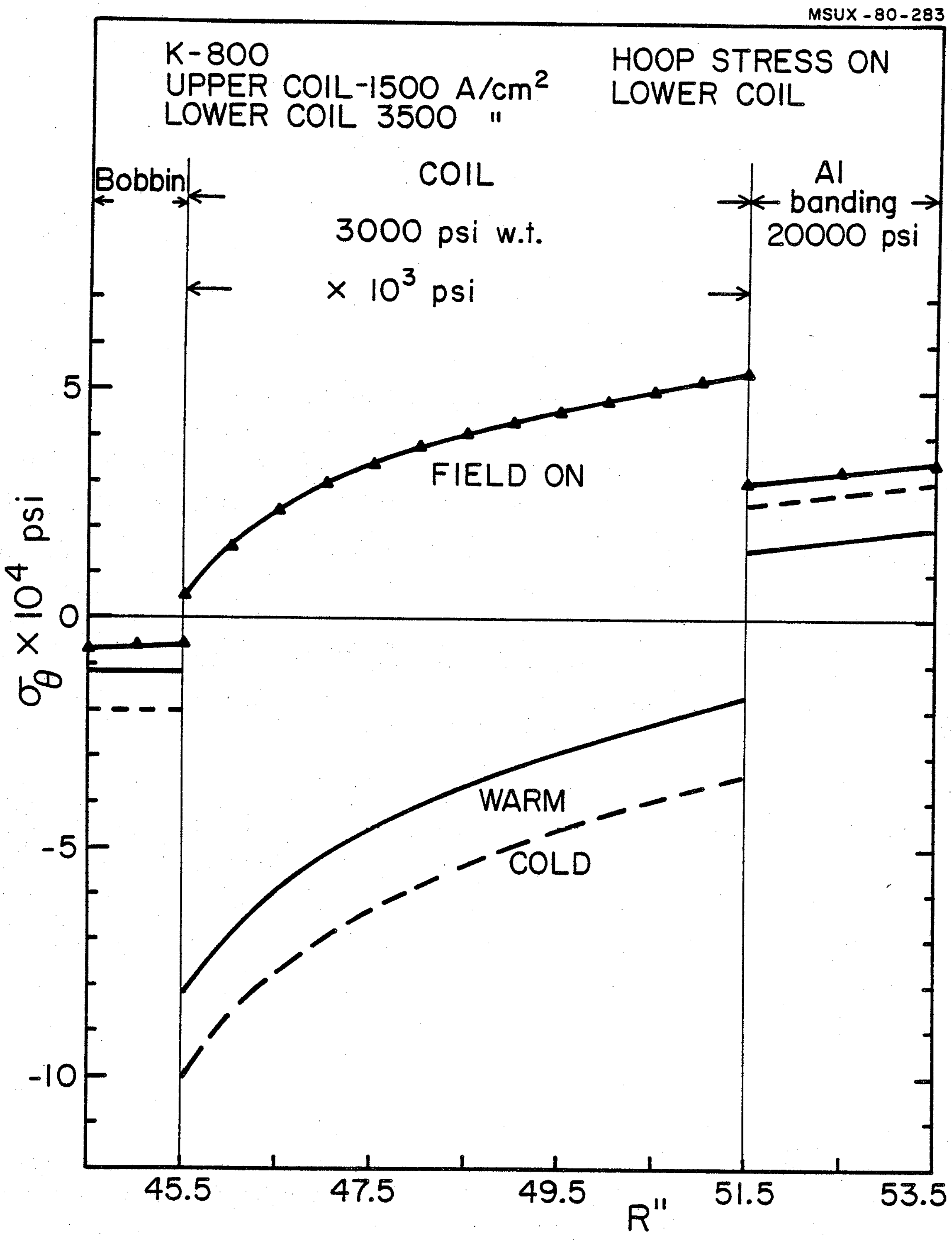
MSUX-80-283
K-800
UPPER COIL-1500 A/cm²
LOWER COIL 3500 "
HOOP STRESS ON
LOWER COIL
Bobbin
COIL
3000 psi w.t.
× 10³ psi
Al
banding
20000 psi
FIELD ON
WARM
COLD
σθ × 10⁴ psi
5
0
-5
-10
45.5
47.5
49.5
51.5
53.5
R"

Figure 14

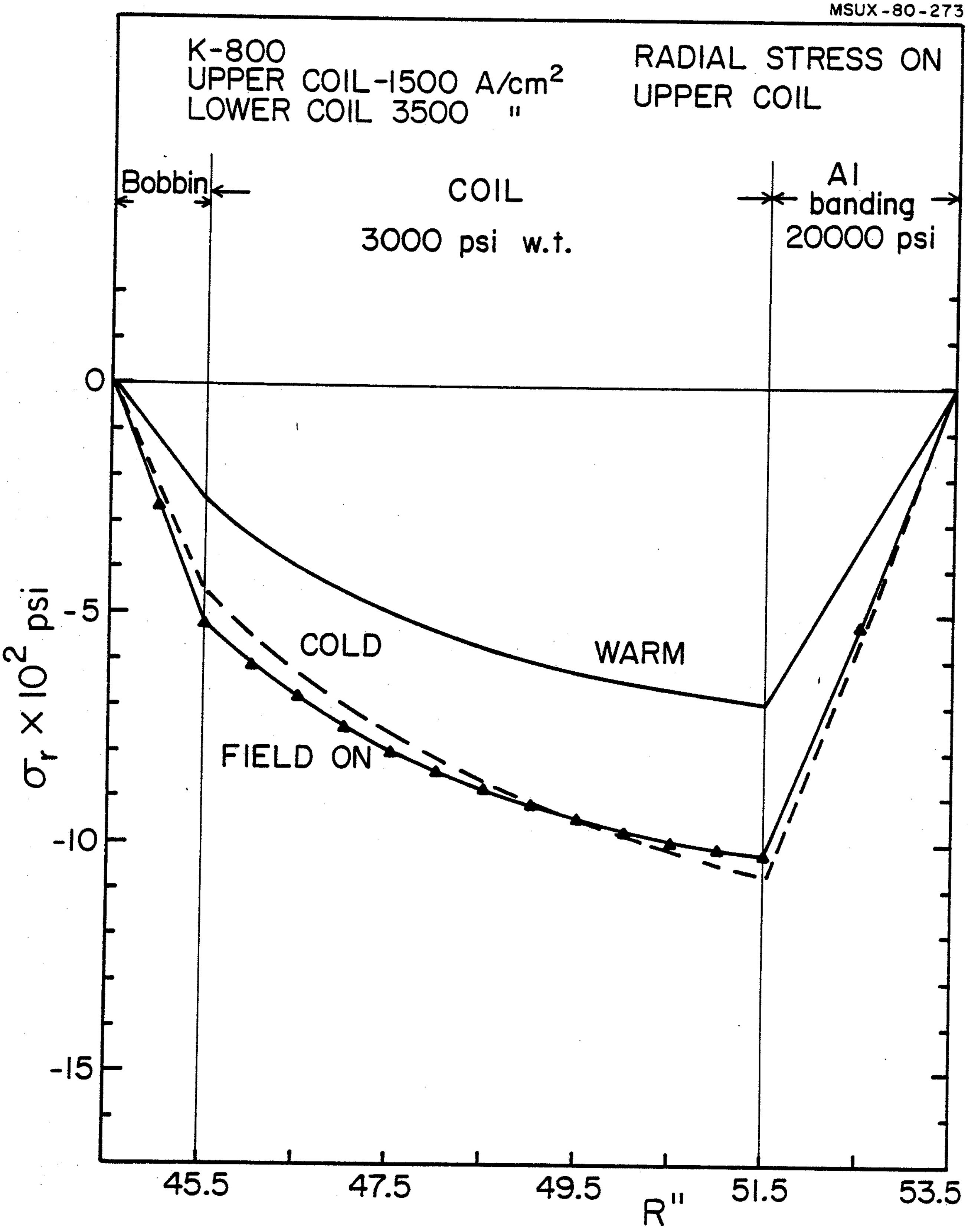
MSUX-80-273
K-800
UPPER COIL-1500 A/cm²
LOWER COIL 3500 "
RADIAL STRESS ON UPPER COIL
Bobbin
COIL
3000 psi w.t.
Al banding
20000 psi
0
-5
-10
-15
σr × 10² psi
COLD
WARM
FIELD ON
45.5
47.5
49.5
51.5
53.5
R"

Figure 15

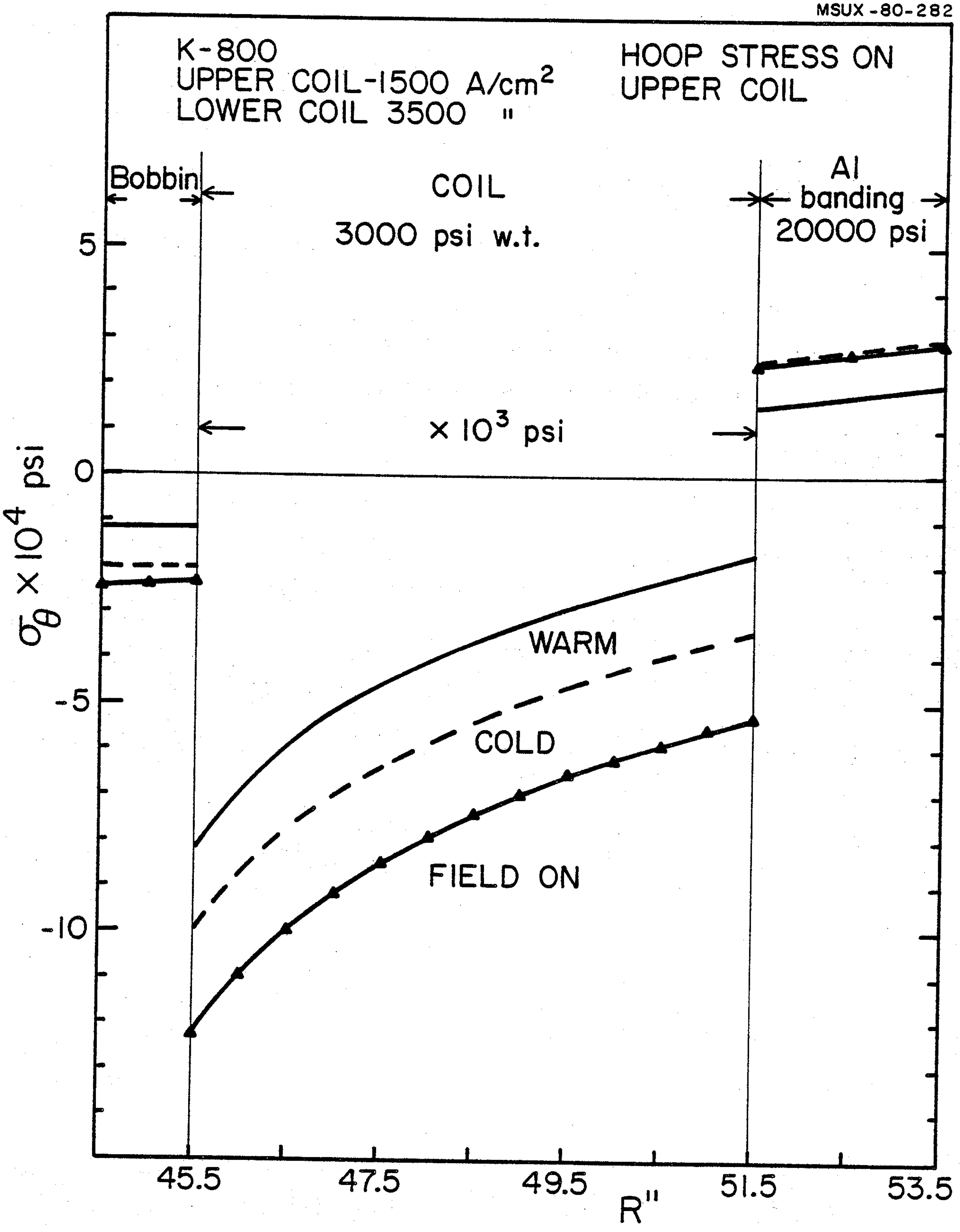
MSUX-80-282
K-800
UPPER COIL-1500 A/cm²
LOWER COIL 3500 "
HOOP STRESS ON
UPPER COIL
Bobbin
COIL
3000 psi w.t.
Al
banding
20000 psi
× 10³ psi
WARM
COLD
FIELD ON
σθ × 10⁴ psi
5
0
-5
-10
45.5
47.5
49.5
51.5
53.5
R"

Figure 16